Probing Weak Molecular Orbital Interactions in Non-Conjugated Diene Molecules by Means of Near-Edge X-ray Absorption Spectroscopy

V. C. Felicíssimo,*,†,‡ A. Cesar,‡ Y. Luo,† F. Gel'mukhanov,† and H. Ågren†

Theoretical Chemistry, Roslagstullsbacken 15, Royal Institute of Technology, S-106 91 Stockholm, Sweden, and Departamento de Química, Universidade Federal de Minas Gerais, Av. Antonio Carlos, 6627, CEP-31270-901, Belo Horizonte, MG, Brazil

Received: November 17, 2004; In Final Form: July 1, 2005

Carbon and oxygen near-edge X-ray absorption fine structure (NEXAFS) spectra of 1,4-cyclohexadiene, *p*-benzoquinone, norbornadiene, norbornadienone, and *cis*-*cis*-[4,4,2]propella-3,8-diene-11,12-dione were calculated by means of Hartree−Fock and hybrid density functional theory using the static-exchange (STEX) approximation. The NEXAFS spectra are used as a probe to identify weak molecular interactions between the two non-conjugated ethylenic π^* orbitals present in these molecules. We show that the X-ray absorption spectrum of 1,4-cyclohexadiene exhibits some particular spectral structures in the discrete energy region that evidence diene through-bond orbital interaction, whereas absorption peaks are identified in the norbornadiene and norbornadienone spectra that indicate effective through-space orbital interactions. The molecular structure of the *cis*-*cis*-[4,4,2]propella-3,8-diene-11,12-dione isomer is such that the indirect through-bond or through-space diene orbital interactions are too weak to be assigned by its C1s NEXAFS spectrum.

1. Introduction

Large molecules often consist of interacting subunits or functional groups. The interactions between localized orbitals of these different functional groups guide many conformational aspects of organic and inorganic molecules. This principle has gradually evolved in the minds of experimentalists and has been widely used in different spectroscopies. Indeed, effects of molecular orbital (MO) interactions are observed influencing, e.g., the ultraviolet (UV) and near-UV spectra, as well as the positions of negative molecular ion resonance states temporarily formed in a low-energy electron−molecule scattering process. Valence photoelectron (UPS) as well as electron momentum spectroscopies (EMS) are also quite useful methods for diagnosing the perturbations caused by molecular interactions in the space of the occupied valence orbitals, whereas electron energy loss spectroscopies (EELS) are sensitive to the empty (virtual) space of molecular orbitals. Photoabsorption in the optical and UV regions contains useful pieces of information to simultaneously map orbital interactions at both spaces of occupied and virtual valence molecular orbitals. In this work, we are concerned with spectral signatures of weak molecular orbital interactions within the virtual valence orbitals of simple nonconjugated diene molecules, as seen from their NEXAFS spectra at the core ionization edges.

Near-edge X-ray absorption fine structures (NEXAFS) spectroscopy measures the electronic transitions from a core orbital localized on a certain atom to a set of vacant molecular orbitals[1] and gives direct information about the atomic contribution of each probed unoccupied molecular orbital. This spectroscopy has a propensity of fingerprinting site-specific excitations for weakly interacting chromophore units that can be identified in a molecule. This characteristic feature leads to the "building block" concept[1−3] that has often served as a useful tool for interpretation of the main features of NEXAFS spectra of larger molecules. The occurrence of such group fingerprints are explained on the grounds of the best dipolar overlap of a tightly localized core orbital, residing close to a particular atomic nucleus, with an empty valence molecular orbital. The interaction between two or more chromophores will perturb the X-ray spectral features (resonances) of the individual groups, shifting their energies and changing their relative intensities. The NEXAFS fingerprinting capability and the "building block" concept, adapted to take into account inter-moiety interactions, could be useful to experimentally identify orbital interactions even in the cases where weak orbital interactions occur. This could be an interesting study case to be explored using the non-conjugated diene class of molecules.

The set of selected molecules for NEXAFS calculations comprises 1,4-cyclohexadiene (CHD), bicyclo[2,2,1]hepta-2,5-diene (norbornadiene, NBD), bicyclo[2,2,1]hepta-2,5-dien-7-one (norbornadienone, NBDO), and *cis*-*cis*-tricyclo[4,4,2,$0^{1,6}$]dodeca-3,8-diene-11,12-dione or *cis*-*cis*-[4,4,2]propella-3,8-diene-11,-12-dione (PPDO). These molecules contain two non-conjugated ethylenic π orbitals that may interact among themselves by long-range through-bond (TB) or through-space (TS) mechanisms. Direct through-space and indirect through-bond effective orbital interactions[4−6] are qualitative molecular orbital concepts originally developed for accounting some spectral subtleties observed in the UV and valence photoelectron spectra of classes of molecules containing two lone pairs or non-conjugated π orbitals. Interactions within the virtual space of molecular orbitals may have an important role in long-range electron transfer process[7] with consequences for chemical reactions and molecular electronics.[8] CHD and NBD are prototypes for the class of molecules with non-conjugated diene groups that interact with each other predominantly by the action of TB or TS mechanisms, respectively. Through-bond hyper-conjugative interaction happens to be dominant in CHD, whereas through-

* Corresponding author. E-mail: viviane@theochem.kth.se.
† Royal Institute of Technology.
‡ Universidade Federal de Minas Gerais.

10.1021/jp044757e CCC: $30.25
Published on Web 08/04/2005

space interaction shapes some UV spectral properties of NBD. Propelladienes, α-diketones, or diazobicyclodienes[5,9] are further examples of molecules containing non-conjugated chromophores displaying TB or TS interactions. Previous experimental UPS,[6] EMS,[10,11] and EELS,[12] and theoretical[13−16] investigations have evidenced TB and TS interactions in CHD and NBD.

In contrast to the weak TS and TB orbital interaction regime of the molecules discussed above, the C1s NEXAFS spectrum of the *p*-benzoquinone (pBQ) molecule has also been calculated. The diene π orbitals present in this molecule are stabilized via a strong conjugative interaction to the two bridging carbonylic groups.

In what follows, in section 2 some details will be given of the utilized computational methods. The results are presented in section 3, where first the C1s NEXAFS spectrum of the pBQ molecule will be considered in order to observe how the extent of the strong diene−carbonyl conjugative π-orbital interaction changes the diene π^* NEXAFS spectral pattern. Next, the changes in the X-ray absorption spectra of the other sampled dienes are analyzed, as the respective orbital interactions are scaled down in strength and switched from TB to TS types. The O1s NEXAFS spectra of pBQ, NBDO, and PPDO are presented and discussed in section 3.4. Our findings are summarized in section 4.

2. Computational Details

The NEXAFS spectra of the CHD, NBD, pBQ, and NBDO were calculated using localized C1s or O1s core-orbitals Hartree−Fock static-exchange (HF-STEX) approximation[17] in the *DALTON* program[18] and gradient-corrected density functional theory (DFT) with full core-hole potential in DeMon codes.[19] For PPDO, only DFT results are presented. In the HF-STEX calculations, we use a 6-311++G** atomic orbital basis for the C, O, and H atoms.[20] This basis set was further augmented by a large diffuse and flexible set of (20s, 18p, 20d)[2,3,17,21] one-electron functions centered at the K-shell core-ionized atom. This double basis set expansion ensures a sufficiently dense orbital space for an adequate description of the discrete pre-edge and continuum parts of the NEXAFS spectrum. The resonances prior to the ionization potential (IP) are convoluted with a Gaussian function with a full width at half-maximum (fwhm) of 0.7 eV, and the continuum is generated by the Stiltjes imaging approach.[17]

In addition to the augmented diffuse basis set, a double basis set technique is employed in the DFT calculations for energy minimization. The PD86 correlation functional by Perdew and Wang[22] and the exchange functional of Becke[23] were selected for all spectral calculations. The ionization potentials, as well as the core excitation energy to the lowest unoccupied molecular orbital (LUMO), were computed using the ΔKohn−Sham scheme. In these calculations, we have used the IGLOO-III triple-ζ basis of Kutzelnigg, Fleischer, and Schindler[24] to describe the core excited atoms and effective core potentials (ECP) for the remaining atoms. We have employed four electron ECPs for carbon and six for oxygen.[19] The spectra were calculated in the full core-hole approach. The energy levels have been calibrated so that the calculated energy of the LUMO coincides with the difference in total energy between the ground state and the core excited state.

All molecular geometries were optimized for their respective electronic ground state at the HF level with a 6-311G** basis set, and these ground-state geometries were then used in all calculations of the core excited spectra.

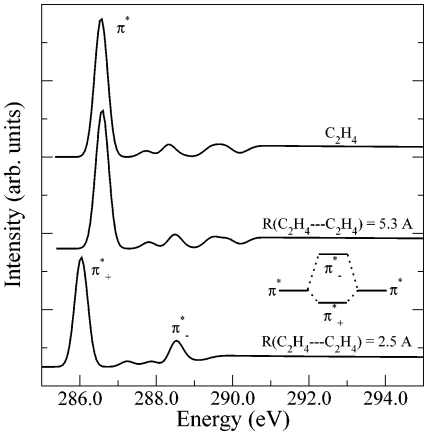

Figure 1. Hartree−Fock calculated C1s NEXAFS spectra of ethylene dimer at different $R[(C_2H_4\cdots C_2H_4)]$ intermolecular distances.

3. Results and Discussion

3.1. Preliminary Considerations. The K shell NEXAFS spectra of monounsaturated organic molecules are, in general, dominated by a first salient structure carrying nearly all the oscillator strength of the K pre-edge region. This structure is assigned as a one-electron transition from the 1s core orbital into the first π^* antibonding molecular orbital. In addition to this prominent peak, the NEXAFS spectra also display structures below and above the core ionization threshold that correspond, respectively, to the filling of higher-lying π^*, Rydberg, and σ^* MOs.[1]

When there exist two or more interacting unsaturated bonds, the first π^* band still remains the most intense one, but it is then often followed by a few more π^* bands of decreasing intensities. As an illustration, the effects of an orbital interaction in a non-conjugated diene group, as seen in a C1s NEXAFS spectrum of an in-plane ethylene dimer model, with the two double bonds lying parallel to each other, were simulated for different diene−diene distances, Figure 1. As the two ethylene molecules approach each other, the interaction within the unoccupied π_1^* and π_2^* orbitals results in a new energy split $\pi_\pm^* = \pi_1^* \pm \pi_2^*$ set of dimer molecular orbitals. The $\pi_-^* \leftarrow$ C(1s) and $\pi_+^* \leftarrow$ C(1s) NEXAFS transitions can be clearly seen in the calculated spectrum for $R[(C_2H_4\cdots C_2H_4)] = 2.5$ Å. This feature will be used to describe the intramolecular interaction in the diene molecules studied here.

To obtain a calculated NEXAFS spectrum of good quality, three main determining electronic factors should be considered: (a) an electron relaxation that will screen a created hole at an atomic site, (b) the initial and final electronic state correlation, and (c) a mutual dynamic response between the excited electron and the $(N-1)$-electron electrostatic potential of the residual ion. The STEX method[17] does not include contributions of the last effect; rather, only a static electron potential of the $(N-1)$-electron ion core is taken into account. The HF method can describe screening relaxation of the valence electron density toward the center with a core hole, but it does not include electron correlation. Electron relaxation and correlation are effects that usually give opposite contributions to the final core-hole ionization potential with, as a rule, the relaxation effect being the dominant factor. This explains the fairly good performance, and limitations, of the HF calculations in recovering the gross features of a NEXAFS spectrum.[2,3,17,21] Improved calculated of NEXAFS spectra will be provided in this work by including electron correlation by means of the DFT method.

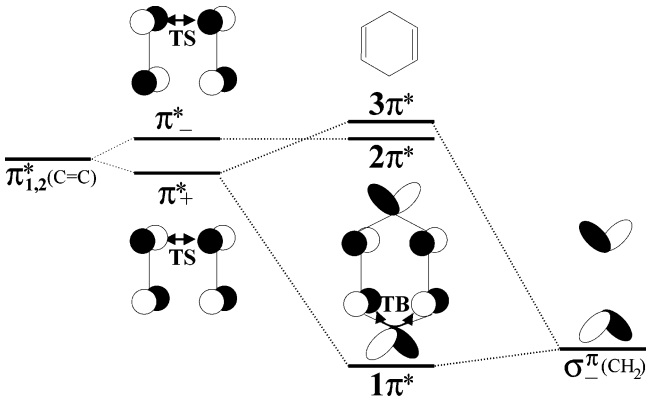

Figure 2. Qualitative scheme of the π^* virtual orbital energy diagram of CHD molecule. The splitting due to the weak through-space (TS) interaction of the π^* ethylenic virtual orbitals is presented on the left side. On the right side, the antibonding pseudo-π orbital of the methylenic groups is shown.

The π^* space of valence virtual orbitals of the selected investigated dienes is formed, in a very simple qualitative approximation, as a linear combination of the ethylenic π^*(C═C) orbitals and, if any, the π^* orbitals of the bridging groups. The symmetry-adapted $\pi^*_\pm$(C═C) diene molecular orbitals are formed as a bonding and antibonding linear combination of the two **1** and **2** unsaturated subunits. Caused by the mutual electrostatic interaction, an energy splitting is expected for the diene $\pi^*_\pm$(C═C) orbitals, as one can see from the scheme of Figure 2. For instance, from an electron transmission spectroscopy (ETS) experiment, the measured $\pi^*_+ - \pi^*_-$ energy splittings were found to be 0.92 and 1.52 eV for CHD and NBD, respectively.[25] In CHD, the TB dominates over the TS interaction, and an π^*_-(C═C) below π^*_+(C═C) inverted energy orbital order is observed. The opposite is found for NBD where the orbital energy order is normal with π^*_+(C═C) below π^*_-(C═C).

3.2. Molecular Structures. The diene molecules under investigation may be considered built up from two 1,2-dehydrogenated ethylene biradical units wired together by two biradical or one tetraradical bridging groups. Within this simple view, a pair of dehydrogenated formaldehyde biradicals or, what is equivalent, two carbon monoxide units "bracket" the diene units, giving the pBQ molecule; two methylene groups can be viewed in CHD, but just one 1,1,3,3-propane and one 1,1,3,3-propan-2-one tetraradical fragments are required to form the NBD and NBDO molecules, respectively. A 1,1,4,4-tetramethyl-2,3-cyclobutadione tetraradical intercalator keeps the two olefinic groups far apart in PPDO. The structures for the CHD, NBD, pBQ, NBDO, and PPDO molecules are sketched in Figure 3, and some selected bond distances and bond angles are given in Table 1.

TABLE 1: DFT Ground-State Optimized Geometrical Parameters of *p*-Benzoquinone (pBQ), 1,4-Cyclohexadiene (CHD), Norbornadiene (NBD), Norbornadienone (NBDO), and [4,4,2]Propella-3,8-diene-11,12-dione (PPDO)[a]

parameters	pBQ	CHD	NBD	NBDO	PPDO
r(C═C)	1.343(0)	1.333(4)	1.335(7)	1.344(0)	1.335(7)
r(C═O)	1.208(4)			1.192(4)	1.200(9)
r(═C−H)	1.074(4)	1.078(1)	1.073(8)	1.072(9)	1.087(2)
r(C−C═)	1.479(6)	1.506(6)	1.545(0)	1.521(9)	1.508(9)
r(X···X)[b]	2.878(6)	3.000(8)	2.244(5)	2.312(8)	2.930(7)
r[(C═C)···(C═C)]	2.529(5)	2.510(6)	2.491(2)	2.495(6)	5.057(5)
∠HCH(CH$_2$)		104.(4)	110.(5)		106.(0)
∠YCH[c]			117.(9)	117.(5)	
∠CYC[c]	117.(5)	112.(9)	92.(0)	93.(8)	90.(3)
∠(C═C)W(C═C)[d]	180.0	180.0	115.(0)	119.(7)	167.(6)
∠(C═C)Z(C═C)[e]					144.(8)
∠H$_2$C···CH$_{ax}$[f]					98.(1)
∠(H$_2$C)CH$_{eq}$[f]					155.(7)

[a]Bond distances are given in angstroms and angles in degree. [a] X is the C═O carbon atom in pBQ, CH_2 in CHD, and PPDO and CH in NBD and NBDO. The $C_1\cdots C_6$ and $(O)C_{11}\cdots C_{12}(O)$ distances in PPDO are 1.578(4) Å and 1.561(2) Å, respectively. [b] Y is the CH_2 bridging carbon atom in CHD and NBD, and the C═O carbon in pBQ, NBDO, and PPDO. [c] W is the middle point along the $H_2C\cdots CH_2$ axis in CHD, $O{=}C\cdots C{=}O$ in pBQ, HC···CH in NBD and NBDO, and $C_1\cdots C_6$ in PPDO. [e] Z is the middle point along the $C_2\cdots C_5$ or $C_{10}\cdots C_7$ axis in PPDO. [f] ax/eq are the axial/equatorial methylenic hydrogen atoms in PPDO.

Inspecting Table 1, we note that the distance between the two ethylenic units, *r*[(C═C)···(C═C)], is shorter in NBD and NBDO than in CHD and pBQ. The ∠CC(H$_2$)C included angle at the apical carbon in NBD and ∠CC(═O)C in NBDO are close to 90°, indicating that the five-membered ring in these molecules is rather strained at that place. The six-membered rings in the PPDO molecule assume an open-book-like conformation, with an opening angle of 144°, giving thus a corrugated shape for the two fused ring *cis*-decaline-like base. The defined mean plane of this base has a ∠(C═C)(C−C)(C═C) bending angle of 167°. Within this conformation, four hydrogen atoms of the methylene groups are placed in an axial position, perpendicular to the base mean plane, and the four others are in an equatorial position, closely lying on the base mean plane. The distance between the two opposite methylene groups within a ring, $r = 2.930$ Å, is approximately the same distance as that found in the CHD molecule.

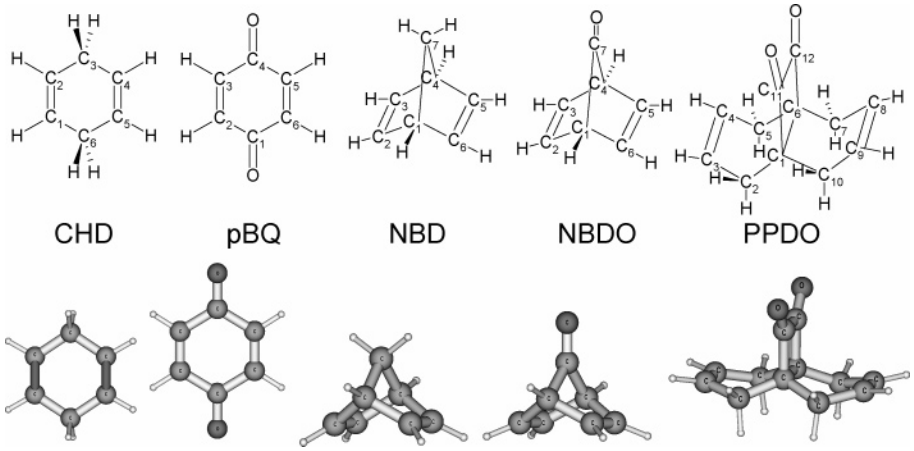

Figure 3. Molecular structures of 1,4-cyclohexadiene (CHD), *p*-benzoquinone (pBQ), norbornadiene (NBD), norbornadienone (NBDO), and *cis*-*cis*-[4,4,2]propella-3,8-diene-11,12-dione (PPDO).

3.3. CK NEXAFS Spectra. 3.3.1. C1s(C═C) Partial NEXAFS Spectra of Non-Conjugated Dienes. The results of the theoretical simulations of the CK and OK shell NEXAFS spectra for the set of selected molecules will be individually detailed in the next sections. Here, we shall be concerned only with the C1s(C═C) partial contribution to the total NEXAFS spectra of non-conjugated dienes, from where spectral structures relevant to the presumed diene orbital interactions should clearly emerge. The carbonyl compounds were appropriately chosen such that an expected contrast shall be made with respect to the strength of the investigated π diene orbital interactions: larger in the pBQ case, because of a strong conjugative interaction of the diene moiety and the two bridging carbonylic groups, and faint in PPDO molecule, where the longest ethylenic−ethylenic distance is observed.

The calculated partial CK(C═C) NEXAFS spectra of the studied dienes are presented in Figure 6a, and the respective assignments are collected in Tables 2 and 3. These partial spectra all have in common a strong first peak, corresponding to a π^* transition, and a weak structure next to the ionization threshold assigned to a σ^*(C−H) ← C1s(C═C) core excitation. Because of the rather localized feature of the C1s core-hole electronic state, the first C1s(C═C) diene π^* NEXAFS transition is found to lie nearly at the same spectral energy position, except for the pBQ case. One additional weak structure, assigned to a second π^* transition, can also be observed for the NBD (286.8 eV) and NBDO (286.6 eV) molecules, while pBQ exhibits two extra π^* peaks at 285.7 eV (strong) and 290.3 eV (weak) energy positions.

According to the qualitative general results of the molecular orbital interaction models, the occurrence of the second (for NBD and NBDO) and third (for pBQ) π^* transitions in the respective simulated C1s(C═C) NEXAFS partial spectra gives clear-cut evidence of a reasonable intra-diene virtual valence orbital interaction in these molecules. This non-conjugated interaction is preserved yet over the influence of a drastic electrostatic potential of a created localized inner-shell core hole. Our theoretical simulations show that the weak second π^* core-hole excitation in NBD and NBDO molecules will lie in a noncongested spectral region of their total NEXAFS spectra such that this will make them most probably amenable to be experimentally observed. No second π^* transition is observed in the ethylenic C1s partial NEXAFS spectra of CHD and PPDO molecules, which thus indicates an apparently vanishing effective diene orbital interaction present there. For the CHD case, an interesting piece of information about the non-conjugated through-bond ethylenic interaction can be seen, however, at its methylenic C1s(CH_2) partial NEXAFS spectrum, as discussed in section 3.3.3 below.

A further corroboration for the interpretation of an interaction within the non-conjugated diene π^* orbitals can be extracted by comparing the carbonyl C1s(C═O) partial NEXAFS spectra of NBDO to the PPDO and pBQ ones, Figure 6b and Tables 2 and 3. The issue here is that two carbonyl groups are interacting strongly with each other in the γ- and α-dicarbonyl pBQ and PPDO molecules, respectively, either by extending the π conjugation over the diene group in the former or by their relative spatial proximity in the latter, but only very weakly, if any, to the diene group in the monocarbonyl NBDO case. Thus, whereas a single C1s(C═O) π^* transition (285.7 eV) can be seen in the NEXAFS partial spectrum of the NBDO molecule, two strong π^* structures can readily be distinguished in the spectra of pBQ and PPDO molecules. This discloses the split feature of the interacting π^* virtual valence orbitals of equivalent unsaturated chemical groups and the capability of an X-ray absorption spectrum to unequivocally display them. The same conclusions can be drawn from the O1s NEXAFS spectra of pBQ, PPDO, and NBDO, Figure 11b, where an extended π conjugation over the two carbonyl groups takes place, and thus, two π^*(C═O) transitions should be observed at pBQ and PPDO O1s NEXAFS spectra but just one for NBDO molecule; see section 3.4.

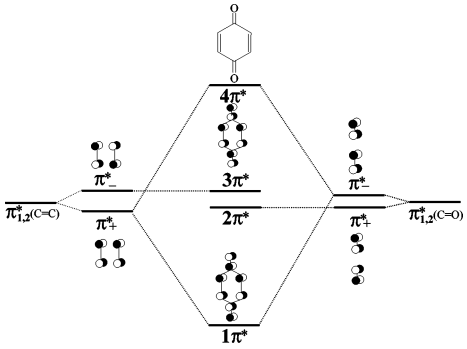

Figure 4. Qualitative scheme of π^* virtual orbital energy diagram of pBQ molecule.

3.3.2. *p*-Benzoquinone. The ground-state **1**π^*(b_{2g}), **2**π^*(b_{3u}), **3**π^*(a_u), and **4**π^* (b_{2g}) molecular orbitals of pBQ can be written as a linear combination of the diene π^* ± (C═C) and the carbonyl π^* ± (C═O) molecular orbitals, as is schematically given in Figure 4. The symmetry is given for the D_{2h} point group, with the pBQ molecule aligned in a right-hand framework with the *x* axis perpendicular to the molecule plane and the *z* axis directed along the two carbonyl groups. The energy differences of these ground-state orbitals were obtained from ETS experiments,[26] and energy separations of 3.26, 0.72, and 2.96 eV are found, respectively, between the consecutive **1**π^*-(b_{2g})−**2**π^*(b_{3u}), **2**π^*(b_{3u})−**3**π^*(a_u), and **3**π^*(a_u)−**4**π^*(b_{2g}) negative ion states. The qualitative orbital energy diagram of the scheme in Figure 4 indicates that **2**π^*(b_{3u}) and **3**π^*(a_u) are quite localized over the carbonyl and diene groups, respectively.

Considering only the **1**−**4**π^* subspace of ground-state molecular orbitals, and disregarding any other weak orbital interaction, only three NEXAFS transitions are expected to occur for each carbon center in pBQ. The C1s(C═O) → **3**π^* and C1s-(C═C) → **2**π^* transitions should not gain intensity in the C1s near-edge energy region, since by symmetry, the **3**π^* and **2**π^* orbitals are kept localized over the ethylenic and carbonylic centers, respectively. This simple view has, however, to be better elaborated for the real cases where effective orbital interactions take place mixing these empty valence orbitals to a set of higher-lying π^*, σ^*, and C(p) Rydberg orbitals. For the purpose of the present analysis, the simplified approximation should nonetheless hold.

An experimental C1s ISEELS (inner-shell electron energy loss spectroscopy) spectrum of pBQ has previously been interpreted in terms of the above **1**−**4**π^* set of valence orbitals.[27] The C1s experimental spectrum of pBQ, reproduced in Figure 5a, shows a pair of intense bands assigned A and B and two other bands with reduced intensities, designated C and D, lying at 283.74 eV (A), 286.00 eV (B), 288.3 eV (C), and 290.7 eV (D). The corresponding C1s(C═C) and C1s(C═O) ionization continua are set at 290.3 and 293.0 eV, respectively. The B band has apparently a larger intensity than the A band, but from its broader width, it can be inferred that it is formed by an overlap of two other bands, B1 and B2. A similar experimental NEXAFS spectrum was obtained for 2,5-dimethyl-1,4-benzo-

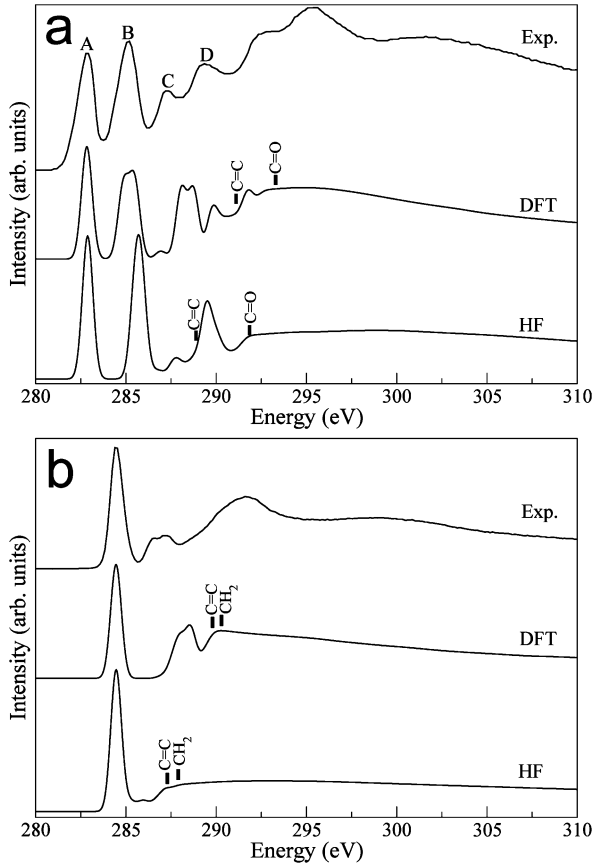

Figure 5. C1s NEXAFS spectrum of (a) *p*-benzoquinone (pBQ) and (b) 1,4-cyclohexadiene (CHD) calculated by HF and DFT methods. The experimental ISEELS (inner-shell electron energy loss spectroscopy) spectrum of pBQ is extracted from ref 27. In both cases, the HF and experimental spectra have been uniformly shifted to coincide with the DFT theoretical first π^* peak energies. The vertical lines mark the onset of the different C1s ionization potentials.

quinone adsorbed on an Ag(111) surface.[28] In this spectrum with improved resolution, the perturbation caused by the two methyl groups makes it possible to clearly identify two transitions at the B energy region. To these spectral structures, the electronic transitions C1s(C═C) → **1**$\pi^*(b_{2g})$, C1s(C═C) → **2**$\pi^*(b_{3u})$, C1s(C═O) → **1**$\pi^*(b_{2g})$, C1s(C═O) → **2**$\pi^*(b_{3u})$, and C1s(C═C) → **4**$\pi^*(b_{2g})$ are assigned to the A, B1, B2, C and D bands, respectively. The C1s(C═O) → **4**$\pi^*(b_{2g})$ transition was proposed to lie about 0.6 eV above the ionization threshold, overlapping there with the σ^*(C−C) resonance.[29]

The HF and DFT calculated C1s NEXAFS spectra of pBQ are shown as the lower and middle curves in Figure 5a, respectively, and the main features are collected in Table 2. These spectra were constructed by adding up the C1s(C═C) and C1s(C═O) partial NEXAFS curves; see Figure 6 for DFT results.

The computed pre-edge HF spectrum of pBQ shows four well-separated bands at 285.8, 288.6, 292.5, and 295 eV, that correlate, respectively, to the A to D bands in the experimental spectrum, Figure 5a. The A and B HF bands are, however, 2.1 and 2.6 eV higher in energy compared to the experimental results, and the HF results are unable to reproduce correctly either the broadening of the B band or the A/B experimental relative intensity ratio. The DFT calculated spectrum, Figure 5a, exhibits the same main bands as in the HF spectrum, but it displays transition energies and relative intensities at the pre-ionization discrete region that are in better agreement with the experimental results. The corresponding A to D four peaks are observed at 283.0, 285.3, 288.1, and 288.9 eV. The width of the band at 285.3 eV is now very well reproduced, but it should be noticed that the intensity ratio of the second to the first bands still disagrees with the experimental value. This discrepancy can perhaps, in part, be referred to the cation one-electron effective STEX potential that is tailored to provide a better description of the intensity and energy position of nonlocal or diffuse orbitals, in that they do not penetrate the core and screen the potential, something that is unaccounted for by STEX. Thus, this leads to energy and intensity that are somewhat too large for a local π^* excitation.[30] Normally, this error can lead to a simple shift of $\leq$1 eV upward in energy.[31]

A characteristic of an electron excitation or ionization from an inner molecular orbital is that the positive hole created in the core induces an electrostatic screening relaxation on the virtual valence orbitals, pulling them down from their original ground-state energy positions, while driving up in energy the core orbital.[1] These effects mostly influence the virtual orbitals with larger amplitudes at the center where the core hole is produced. Overall, these relaxation processes force a set of virtual orbitals to stay below the ionization threshold and condense most transition oscillator strength to the localized virtual orbitals of low energy. Because of the localization of the electronic density, changes may be expected on the initial ground-state orbital energy ordering, and the core-hole molecular orbitals may not display the full group symmetry of the framework of the molecular nuclei anymore. It is therefore interesting to verify the extent of change of the ground-state orbital energy diagram of pBQ upon a C1s(C═C) or C1s(C═O) core electron excitation.

By taking into account the core-hole screening relaxation, the virtual molecular orbital ordering of the pBQ molecule, as seen by the respective C1s(C═C) and C1s(C═O) DFT NEXAFS spectra, is obtained as shown in Figure 9. This energy ordering can be disclosed as follows: Considering the separated C1s channels, the DFT C1s(C═O) partial spectrum gives a 3.1 eV energy separation for the (C1s → **2**π^*) and (C1s → **1**π^*) transitions. This agrees very well with the value of 3.26 eV from the ETS experiments.[26] This means that these two molecular orbitals will screen the C1s core hole nearly by the same amount, and consequently, the qualitative orbital diagram for the final C1s(C═O) core-hole excited state will have the **1**π^*−**2**π^* relative energy position as that found in the energy diagram of the corresponding negative ion electronic states. Also, this 3.1 eV separation is approximately the gain in stabilization energy by the π^*_-(C═O)orbital upon the π^*_-(C═O) + π^*_+(C═C) diene−dicarbonyl interaction (Figure 4). Now with regard to the C1s(C═C) partial spectrum, the DFT energy gap found for the π^* peaks, as compared to the ordering of the negative ion orbital energies, looks somewhat unexpected. This result is reconciled if a strongly screened C1s(C═C) final core-hole state with inverted $\pi^* \pm$ (C═O) to $\pi^* \pm$ (C═C) energy positions is recognized as shown in Figure 9. With this inversion, the relative orbital mixing of the **1**π^* and **4**π^* orbitals will be switched, and they will become more π^*_+(C═C)- and π^*_-(C═O)-like, respectively.

The conclusions that can be drawn from the pBQ NEXAFS results are that strongly interacting diene groups develop two intense π^* bands at the pre-edge region because of resonant conjugation with the pair of carbonylic π^* orbitals. An extra weak peak may occur lying very close to the ionization threshold, or it might even pass into the continuum. The energy positions of these bands are quite dependent on the strength of the C1s(C═C) core-hole screening that may drastically modify

TABLE 2: HF and DFT C1s NEXAFS Transition Energies and C1s Ionization Potentials (IP) of *p*-Benzoquinone (pBQ)

C1s transition energies (eV)						
partial spectra						
HF		DFT				
C=C	C=O	C=C	C=O	total DFT spectrum	exp[a]	assignments
285.8		283.0		283.0	283.74	π^*(C=C)
288.8	288.5	285.7	284.7	285.3	286.00	π^*(C=O) + π^*(C=C)
	292.5		287.8	288.1	288.3	π^*(C=O)
		289.1		288.8		σ^*(C−H; C=C)
290.6		290.3		290.3	290.7	π^*(C=C)
291.8		291.1		291.1	290.3	IP (C=C)
			292.0	292.0		σ^*(C−C; C=O)
	294.8		293.3	293.3	293.0	IP (C=O)
					293.6	σ^*(C−C; C=C) + π^*(C=O)
					296.2	σ^*(C−C; C=C) + σ^*(C−C; C=O)
	303				303	σ^*(C−C; C=O)

[a] Experimental results from ref 27.

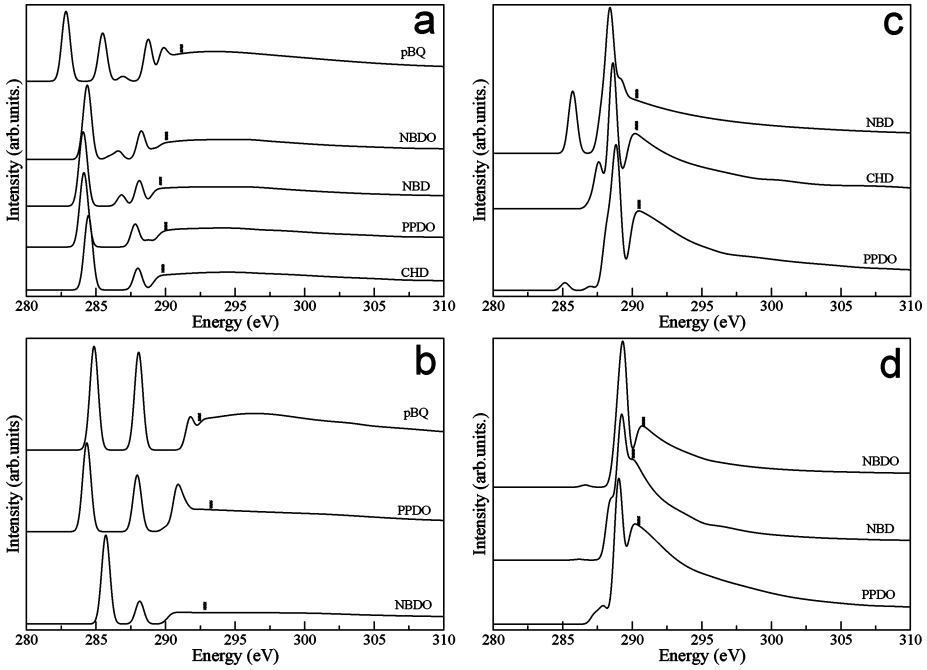

Figure 6. Partial NEXAFS spectra with core hole in (a) C1s (C=C), (b) C1s (C=O), (c) C1s (CH_2), and (d) C1s (CH or CC_4) calculated by the DFT method. The vertical broken lines mark the onset of the different C1s ionization potentials.

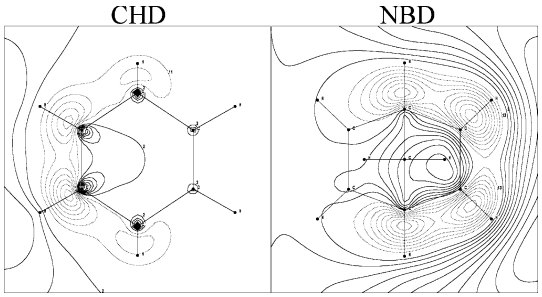

Figure 7. Virtual valence σ^* molecular orbitals of C1s core-ionized state of 1,4-cyclohexadiene (CHD) and norbornadiene (NBD). These orbitals are localized over the ethylenic fragment where a C1s core hole has been created.

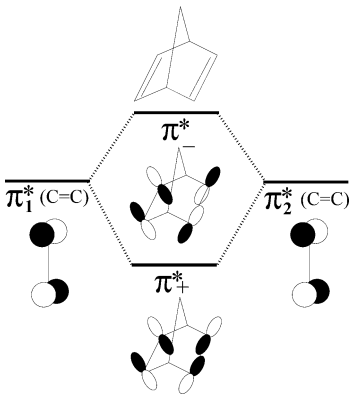

Figure 8. Qualitative scheme of π^* virtual orbital energy diagram of NBD molecule.

the normal orbital correlation diagram of the ground state. All these effects are expected to have images at the weakly interacting non-conjugated diene molecules treated in the next section.

3.3.3. 1,4-Cyclohexadiene (CHD). The NEXAFS spectrum of 1,4-cyclohexadiene can be interpreted as a weak interacting diene system that is a limiting case of the pBQ molecule. The π^* group of base molecular orbitals relevant for interpreting the C1s NEXAFS spectrum of CHD, Figure 5b, can be obtained as a linear combination of the diene π^*_+(C=C; b_{2g}) and methylene $\sigma^{\pi}_-(CH_2)$ orbitals and the diene unmixed π^*(C=C; a_1) orbital. The symmetry-adapted hyper-conjugative π-like

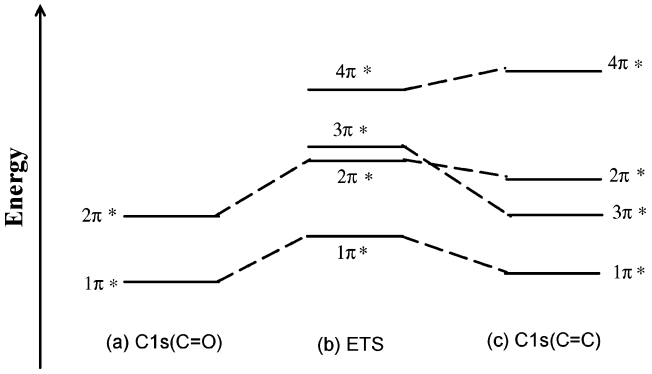

Figure 9. Qualitative virtual orbital energy diagram for pBQ molecule: (a) and (c) ordering observed from the C1s(C═O) and C1s-(C═C) NEXAFS partial spectra, respectively, and (b) from negative ion electron transmition spectroscopy (ETS).

$\sigma^{\pi}_{-}(CH_2) = \sigma^{\pi}_{1}(CH_2) - \sigma^{\pi}_{2}(CH_2)$ orbital, constructed as a negative linear combination of the two σ(C—H) bonding orbitals of each methylene unit, is introduced in order to promote the π* conjugation throughout the six-membered ring;[4] see Figure 2. By symmetry, the diene and methylene π*-orbital interaction occurs by mixing the π^{*}_{+}(C═C) and $\sigma^{\pi}_{-}(CH_2)$ orbitals. It should be noted that $\sigma^{\pi}_{-}(CH_2)$ is a doubly occupied molecular orbital in the electronic ground-state configuration of the CHD molecule, which means that the σ^{π}_{-} orbitals are not really active in a NEXAFS process, where only empty or half-filled atomic or molecular orbitals are mapped upon a core electron excitation. However, the hyper-conjugative interaction mediated by these orbitals will, by orthogonality, induce polarization of the π^{*}_{+}(C═C) virtual orbital that may be sufficient to indirectly change the relative positions and intensities of the π^{*}_{+}(C═C) NEXAFS resonance; see Figure 2.

The calculated HF and DFT NEXAFS spectra of the CHD molecule are shown in the lower and middle curves of Figure 5b, respectively. We can see that the pre-edge HF spectrum shows one very strong π*(C═C) excitation band at 287.4 eV and three others with very weak intensities at 288.2, 289.0, and 289.5 eV. The inclusion of the B3LYP/DFT correlation effect dramatically redistributes the C1s oscillator strengths of CHD below and above the ionization threshold, now describing much better the NEXAFS pre- and post-edge intensity distributions as compared to the EELS experimental results.[32] This redistribution, which also was observed for the pBQ case, markedly increases the oscillator strength at the post-edge region and raises the intensity of several discrete pre-edge peaks. Besides the stronger π* transition observed at 284.5 eV, two medium-intensity bands are seen at 288 and 288.5 eV, and they are readily assigned as C1s core excitations into the mixed-valence/Rydberg π*(CH_2) and valence σ*(C—C; CH_2) virtual orbitals of the methylene groups, respectively. Discrete π*(CH_2) resonances below the ionization potential threshold have been discussed and assigned in the K-shell excitation of cyclic hydrocarbons.[29] The hyper-conjugation at these bridge groups provides the observed enhanced Cp_{π} orbital oscillator strengths, being more effective along the methylene C—C single bond.

A spectral signature of an orbital interaction between the ethylenic groups of CHD is the band at 288.5 eV, Figure 5b. The reason for this is appreciated more by inspecting the CHD partial C1s(C═C) and C1s (CH_2) spectra, shown in Figure 6a, bottom line, and Figure 6c, middle line, respectively.

First of all, the C1s(C═C) partial spectrum shows the main π* peak at 284.5 eV and a weak band at 288 eV corresponding to a C1s core to σ*(C—H; C═C) excitation. The latter peak is seen at the calculated partial C1s(C═C) NEXAFS spectra of all the considered molecules here. A contour plot of the empty σ*(C—H; C═C) orbitals at the localized ethylenic C1s core-ion state is given in Figure 7 for CHD and NBD molecules. Previous C1s inner-shell single-excitation static-exchange calculations have given a discrete σ*(C—H) peak below the ionization threshold for the ethylene molecule;[33] see also ref 34. In a more recent investigation, Zhu et al.,[35] on the basis of their multiple-scattering cluster and discrete variational X_{α} calculations, argue that this resonance should be placed above the ionization potential. This disagreement may be caused by the lack of a proper description of the Rydberg orbital space in their computations and a correct admixture to the valence σ*(C—H) orbital thereafter. Also, the electronic relaxation contribution to the virtual orbitals due to the localized character of the C1s core hole possibly has a weight on these results.

The peak at 288 eV is hidden behind the structures corresponding to the C1s(CH_2) excitations in the total NEXAFS spectrum (see below) and contributes to make the relative intensity ratio of 288 and 288.5 eV bands stay about 0.9:1. No peak that could disclose a direct non-conjugated diene interaction is seen in the partial C1s(C═C) NEXAFS spectrum. On the other hand, the C1s(CH_2) partial spectrum of CHD shows a pair of resonances at 287.5 and 288.6 eV, just below the ionization threshold with a relative intensity ratio of about 1:3. The higher intensity of the second peak indicates that the virtual molecular orbital reached by the C1s core excitation has a larger C(p_{π}) contribution. The first of these resonances corresponds to a weak C1s → π*(CH_2)transition, while the most intense peak is assigned to a C1s → σ*(C—C; CH_2) excitation. The σ*(C—C; CH_2) transition is normally found lying in the continuum above the IP(CH_2) ionization potential in saturated hydrocarbons.[1,33−35] In the CHD NEXAFS spectrum, it has, however, been pushed down below the ionization threshold because of the hyper-conjugative stabilization interaction of the methylene C(p_{π}) orbital to the diene π(C═C) system. Indeed, in comparison to the experimental C1s NEXAFS spectra of the nonplanar cyclohexane (chair conformation) and cyclohexane molecules, where the σ^{π}(C—H; CH_2) hyper-conjugative orbital interaction is inoperative, just one single π*(CH_2) structure at 2.7 and 2.6 eV below the respective ionization potential is observed.[29] Therefore, the hyper-conjugative interaction in the CHD molecule can be established by the medium-intensity σ*-(C—C; CH_2) resonance at 288.5 eV, pushed 1.3 eV below the IP(C═C)ionization potential.

3.3.4. Norbornadiene (NBD) and Norbornadienone (NBDO). Turning to NBD and NBDO, it is first recognized that a direct diene orbital interaction can be made possible in these molecules by the relative tilting angle of the π_1(C═C)/π_2(C═C) and π^{*}_{1}(C═C)/π^{*}_{2}(C═C) molecular orbitals; see scheme of Figure 8.

The HF NEXAFS spectrum of NBD, Figure 10b, follows the general pattern already seen in the CHD spectrum: One very strong π*(C═C) peak at 286.8 eV dominates the whole pre-edge region, and two discrete bands with low intensities at 288.3 and 289.3 eV can be spotted. The most prominent of these two weak bands is a σ*(C—C; CH_2) transition, while the other has contributions from C1s(C═C) to the second π* orbital transition and some residual π*(CH_2) and σ*(C—H; C═C) oscillator strengths. The σ*(C—C; CH_2) transition gains intensity from the strained structure of the apical methylene group that pulls down the antibonding σ*(C—C) orbital from the continuum. A similar effect is observed in the C1s excitation spectra of small $n = 3$, 4, 5, and 6 cyclic saturated hydrocarbons.[29,36]

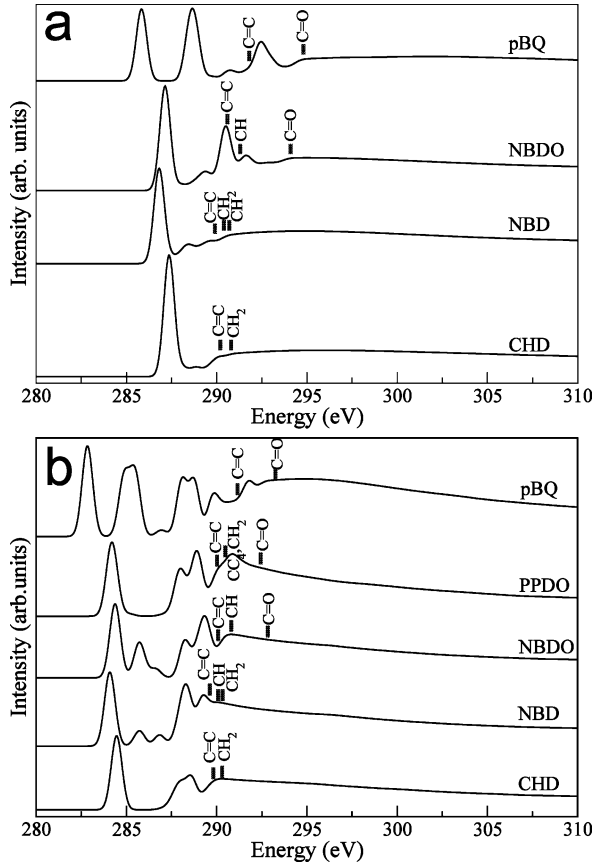

Figure 10. C1s NEXAFS spectra of 1,4-cyclohexadiene (CHD), norbornadiene (NBD), norbornadienone (NBDO), *p*-benzoquinone (pBQ), and [4,4,2]propella-3,8-diene-11,12-dione (PPDO) calculated by HF (a) and DFT (b) methods. The vertical broken lines mark the onset of the different C1s ionization potentials.

A different scenario is seen in the NBDO C1s pre-edge NEXAFS spectrum. Two strong peaks are now observed at 287.1 and 290.5 eV and three others with weak intensities at 288, 289.3, and 291.6 eV. If the building block approximation is considered, the individual contributions to the whole spectrum from the diene and carbonyl groups become apparent. The first peak thus corresponds to the recurrent diene π^*(C═C) transition, whereas the second one, with about half of the intensity of the former, is a C1s(C═O) → π^*(C═O) transition. The medium-intensity peak at 289.3 eV is a σ^*(C−C; C═C) transition, and the other, as analogously observed in NBD, is a C1s(C═O) core excitation into the σ^*(C−C; CH_2) orbital. This transition is calculated to lie, respectively, 2.1 and 2.5 eV below the C1s-(CH_2) ionization potential in the NBD and NBDO molecules. This can be compared with gas-phase cyclopropane where this peak occurs with the term value of 1.6 eV.[29]

The NBD and NBDO DFT NEXAFS spectra are shown in Figure 10b, and their main features with the respective assignments are presented in Table 3. As already noticed for the pBQ and CHD cases, the electron correlation effect redistributes more correctly the C1s NEXAFS spectral oscillator strengths below and above the ionization threshold. The detailed C1s partial spectra of these molecules can be seen in Figure 6a−d. The partial C1s(C═C) spectra of CHD, NBD, and NBDO look quite alike; besides the stronger π^*(C═C) transition peaking at about 284 eV, a medium-intensity peak σ^*(C−H;C═C) arises at about 288 eV. Differently from the CHD case, a second π^*(C═C) weak peak is developed at 286.8 eV (NBD) and 286.5 eV (NBDO) in the spectra of these bicyclo molecules. These structures are readily recognized as weak (NBD) or a shoulder (NBDO) in the respective total C1s NEXAFS spectra and are identified as direct X-ray absorption spectral evidence of a through-space interaction mechanism of the non-conjugated diene functional group.

TABLE 3: DFT C1s NEXAFS Transition Energies and C1s Ionization Potentials (IP) of 1,4-Cyclohexadiene (CHD), [4,4,2]Propella-3,8-diene-11,12-dione (PPDO), Norbornadiene (NBD), and Norbornadienone (NBDO)

	C1s transition energies (eV)					
	partial spectra				total	
molecule	C═C	CH_2	CH	C═O	spectrum	assignments
CHD	284.5				284.5	π^*(C═C)
	288.0	287.5			288.0	π^*(CH_2) + σ^*(C−H; C═C)
		288.6			288.5	σ^*(C−C; CH_2)
		289.8			289.8	IP (C═C)
	290.3				290.3	IP (CH_2)
NBD	284.1				284.1	π^*(C═C)
		285.7			285.7	π^*(CH_2)
	286.8				286.8	π^*(C═C)
	288.1	288.4	288.5		288.3	σ^*(C−H; C═C) + σ^*(C−C; CH_2) + σ^*(C−H; CH)
			289.3		289.3	σ^*(C−C; CH)
	289.6				289.6	IP (C═C)
			290.1		290.1	IP (CH)
		290.3			290.3	IP (CH_2)
NBDO	284.4				284.4	π^*(C═C)
				285.7	285.7	π^*(C═O)
	286.6				286.5	π^*(C═C)(shoulder)
	288.2			288.1	288.3	σ^*(C−H; C═C) + σ^*(C−C; C═O)
			289.3		289.3	σ^*(C−C; CH)
	290.1				290.1	IP (C═C)
			290.8		290.8	IP (CH)
				292.8	292.8	IP (C═O)
PPDO	284.1			284.3	284.2	π^*(C═C) + π^*(C═O)
		285.2				π^*($CH_2[H_{ax}]$)
	287.8	288.1		288.0	288.0	π^*(C−H; C═C) + π^*(C═O) + π^*($CH_2[H_{eq}]$)
		288.8	289.1		288.9	σ^*(C−C; CH_2) + σ^*(C−C; $C(C_4)$)
	290.0				290.0	IP (C═C)
			290.5		290.5	IP ($C(C_4)$)
		290.5			290.5	IP (CH_2)
				290.9	290.9	σ^*(C−C; C═O)
				292.4	292.4	IP (C═O)

Finally, after inspecting the apical bridging C1s partial NEXAFS spectra of NBD and NBDO, the 285.7 eV π^*(CH_2) and 288.3 eV σ^*(C−C; CH_2) ethylenic as well as the 285.7 eV π^*(C═O) and 288.3 eV σ^*(C−C; C═O) carbonylic core transitions gain intensity and are red-shifted below their respective C1s ionization potentials because of the strained bonding structure at the apical carbon atom. The DFT calculated σ^*(C−C; CH_2) and σ^*(C−C; C═O) NEXAFS peaks of CHD, NBD, and NBDO lie at the same energy position. This indicates an equivalent C_p orbital hybridization occurring at the methylenic and carbonylic carbon atoms in this set of molecules. This effect is also seen at the 289.3 eV σ^*(C−C; CH) resonance of the methylinic C1s NEXAFS partial spectra of the NBD and NBDO molecules; see Figure 6d. On the other hand, a 2.3 eV energy shift is observed for the π^*(CH_2) peak of NBD as compared to the same transition in CHD. This large shift is caused by the quite tensioned C−C−C bond at the methylenic moiety (see Table 1) that perturbs the normal sp^3 hybridization at the apical carbon atom. This interpretation is corroborated

TABLE 4: HF and DFT O1s NEXAFS Transition Energies and Ionization Potentials (IP) of *p*-Benzoquinone (pBQ), Norbornadienone (NBDO), and [4,4,2]Propella-3,8-diene-11,12-dione (PPDO)

Transition Energies (eV)								
pBQ				NBDO			PPDO	
HF	DFT	exp[a]	assignments	HF	DFT	assignments	DFT	assignments
531.1	529.4	529.9	**1**π^*(C═O)	534.3	531.2	**1**π^*(C═O)	529.7	**1**π^*(C═O)
536.0	533.1	533.2	**2**π^*(C═O)		533.4	p_σ(C−O)	533.9	**2**π^*(C═O)
537.3	537.7	537.5	IP	536.1	536.4	p_σ(C−O)	535.3	p_σ(C−O)
	538	538.2	**3**π^*(C═O)	537.3	537.4	IP	537.5	IP
	543.4	542.7	σ^*(C−O)					

[a] Experimental NEXAFS results for pBQ from ref 27.

by noting that the 285.7 eV π^*(C═O) excitation localized on the bridging carbon in the NBDO molecule resides at the same energy position as the $\pi^*(CH_2)$ transition in NBD.

3.3.5. [4,4,2]Propella-3,8-diene-11,12-dione (PPDO). To clarify a bit further the above results, the DFT C1s NEXAFS spectrum of the PPDO molecule was calculated. The cis-cis isomer of this molecule is such that the two C═C bonds are forced to stay 5.06 Å apart. This distance completely prevents an effective direct diene orbital interaction from taking place.

The DFT C1s NEXAFS spectrum of PPDO can be seen in Figure 10b. In this spectrum, the three strong bands, one at 284.2 eV due to a π^*(C═C) transition and a pair of σ^* bands at the 288 and 299 eV energy region, mirror the NEXAFS spectra of the other CHD, NBD, and NBDO diene molecules. Differently from NBD and NBDO, but analogously to the CHD case, no discrete structures are developed between the first PPDO π^*(C═C) and the group of σ^* transitions. Also, a broadened band seems to gain intensity just above the C1s(C═C) ionization continuum, at 290.9 eV. The assignments of these bands to their respective core excited electronic transitions are straightforwardly made by inspecting the four different partial C1s NEXAFS spectra of PPDO, shown in Figure 6a,b.

First of all, the unexpected lack of the carbonyl first π^*(C═O) transition, clearly identified in the pBQ and NBDO spectra but not seen in the PPDO spectrum, is readily understood by noting the 1.4 eV shift to lower energy between the C1s-(C═O) → π^*_+(C═O) transitions in PPDO and NBDO. This shift, caused by a π^*_1(C═O) ± π^*_2(C═O) orbital mixing of the two carbonyl centers of the α-diketone functional group, is sufficiently strong to make the C1s(C═C) → π^*_+(C═C) and C1s(C═O) → π^*_+(C═O) bands nearly overlapping at about 284.2 eV in the NEXAFS spectrum of PPDO. The C1s(C═O) → π^*_-(C═O)transition is pushed up in energy and is found at 288.0 eV, giving therefore a $\pi^*_+ - \pi^*_-$ splitting of 3.7 eV. To compare, the $\pi^*_+ - \pi^*_-$ orbital splitting on the 1,2-cyclobutadione has been measured at <2.9 eV by ETS experiments,[37] where $^2\Pi_+$ is observed to be a rather stable negative ion molecular state. The PPDO C1s(C═C) partial spectrum repeats the structures already found in the C1s(C═C) spectrum of CHD, and there are no spectral hints that could point out the presence of a diene orbital interaction. Finally, in the PPDO C1s(CH_2)-partial spectrum, a very weak peak is seen at 285 eV that corresponds to a core excitation into the methylenic $\pi^*(CH_2\text{-}(H_e))$ antibonding orbital with the hydrogen atom in an equatorial position. The most intense axial $\pi^*(CH_2(H_a))$ transition overlaps from the left flank to the σ^*(C−C; CH_2) peak at 288.9 eV. In the total NEXAFS spectra, these pieces of information are overshadowed by the much stronger π^*(C═C) and σ^*(C−C; C═O)transitions lying at the same energy position. Altogether, we find that the NEXAFS spectrum of the PPDO diene molecule can completely be described by a simple sum of the partial subspectra of its noninteracting constituent fragments, without any particularly spectral structure being isolated that could highlight an orbital interaction within the diene or diene-α-diketone functional groups.

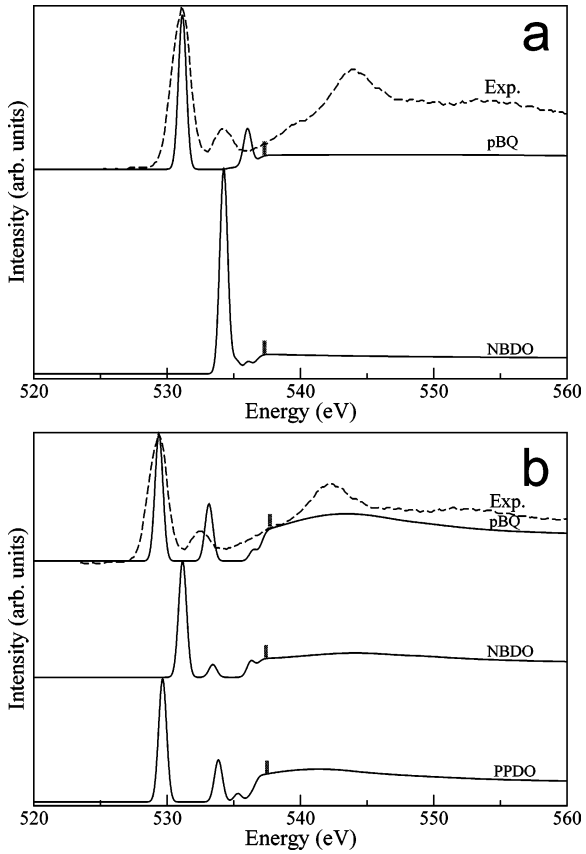

Figure 11. O1s NEXAFS spectra of *p*-benzoquinone (pBQ), norbornadienone (NBDO), and [4,4,2]propella-3,8-diene-11,12-dione (PPDO) calculated by HF (a) and DFT (b) methods. The experimental ISEELS spectrum[27] is shifted to get the same position as the first peak in the theoretical spectrum.

3.4. OK NEXAFS Spectra of *p*-Benzoquinone (pBQ), Norbornadienone (NBDO), and [4,4,2]Propella-3,8-diene-11,-12-dione (PPDO). The pBQ, NBDO, and PPDO O1s transition energies and ionization potentials calculated by Hartree−Fock and DFT methods are presented in Table 4. The monocarbonyl NBDO molecule is expected to produce the simplest O1s NEXAFS spectrum, while additional π^* absorption bands, caused by the strong π-conjugated electronic system, are anticipated to be seen in the α- and γ-dicarbonyl PPDO and pBQ spectra.

The HF O1s NEXAFS spectrum of pBQ (Figure 11a) shows two distinct peaks at 531.1 and 536.0 eV in the pre-ionization region, assigned to the O1s → **1**$\pi^*(b_{2g})$ and O1s → **2**$\pi^*(b_{3u})$ transitions, respectively. Note that the energy position of the center of these two peaks, 533.6 eV, nearly compares with the

HF energy position of the corresponding π^* transition in the NBDO molecule (see below), and therefore, HF stabilization/destabilization energies of 1.7 and 3.2 eV are obtained for the pBQ $\pi^*_{\pm}$(C═O) molecular orbitals, respectively. The inclusion of the correlation energy makes the O1s NEXAFS/DFT peaks shift downward in energy, to 529.4 and 533.1 eV. These values compare very well with the experimental results[27] and also reduce their energy splitting to 3.7 eV (to be compared with 3.1 eV as obtained at the C1s(C═O) DFT NEXAFS spectrum). The O1s as well as the C1s NEXAFS/DFT spectra, as compared to the experimental ones, do not show a perfect intensity ratio for the two first π^* bands; in both O1s and C1s(C═O) spectra, the second π^* transition gains more intensity relative to the first π^* peak in the simulated DFT calculation. The reason for these disagreements can be traced to the lack of a combined correct relaxation of the virtual orbital space and the static core potential upon the C1s and O1s to π^* transitions.

Another feature is distinguished in the continuum region of the DFT O1s NEXAFS spectrum: A bump with considerable intensity is observed peaking at about 543.4 eV. This broad structure corresponds to σ^*(CO) and to a medium-intensity O1s $\rightarrow$ **4**π^*(b_{2g}) transition. Experimentally, equivalent spectral structures are observed at 542.7 and 538.2 eV, respectively. As shown in Figure 11b, the second (533.1 eV) and third (538.2 eV) π^*(C═O) DFT bands gain much more intensity than in the experimental spectrum. This inadequacy again originates in the employed nonpolarized STEX potential that precludes a flexible oscillator strength distribution among the virtual molecular orbitals.

The O1s NEXAFS spectrum (Figure 11b) of PPDO can now be straightforwardly interpreted. The two more intense peaks observed in the pre-ionization region, at 529.7 and 533.9 eV, correspond to the O1s $\rightarrow$ **1**π^* and O1s $\rightarrow$ **2**π^* transitions; the barycenter of these bands is 531.8 eV. A 4.2 eV π^*_+(C═O)$-$$\pi^*_-$(C═O) energy splitting thus is obtained, slightly larger than the splitting found in pBQ. It is remarkable that the π^*_+(C═O)$-$$\pi^*_-$(C═O) splittings of the virtual orbitals observed by means of the NEXAFS transitions are much larger (in the case of pBQ molecule, it is 1 order of magnitude larger) than the π_+(C═O)$-$$\pi_-$(C═O) splittings of the occupied molecular orbitals observed in the photoelectron spectrum. The electronic screening effective in the O1s core-hole states is responsible for this effect. Aside from these two bands, another weak peak is observed below the ionization threshold, at 535.3 eV, that has an equivalence to the 536.4 eV p_σ transition in NBDO. Finally, above the ionization onset, the broad σ^*(C$-$O) transition is seen at 541 eV.

The NDBO DFT O1s NEXAFS spectrum, Figure 11b, shows a strong π^*(C═O) peak at 531.2 eV and two other low-intensity transitions before the ionization onset, assigned to O1s core excitations into low-lying p_σ oxygen orbitals oriented along the C$-$O bond. The pre-ionization region of this spectrum resembles several theoretical ketone NEXAFS spectra reported in ref 21 and also the experimental spectrum of propanone (acetone).[27] Therefore, no orbital perturbation is identified in the empty set of the molecular orbitals of this molecule that could indicate an interaction between the π orbitals of the carbonyl and diene centers. Finally, we note that the strongest NBDO π^*(C═O) peak at 531.2 eV keeps a notable correspondence to the center of the two π^* bands at 531.3 and 531.8 eV in the DFT O1s spectrum of the pBQ and PPDO molecules, respectively.

The pBQ and PPDO molecules show two characteristic intense NEXAFS O1s $\rightarrow$ π^* transitions, a feature not repeated in the corresponding NBDO spectrum, where only a single intense π^* transition is seen in the pre-ionization region. The electronic structures of the pBQ and PPDO molecules are such that an extended π conjugation over the two carbonyl groups takes place and results in two NEXAFS π^*(C═O) transitions. As a result of this interaction, the π^*_+(C═O) and π^*_-(C═O) virtual molecular orbitals are split in energy as the respective barycenters, nearly coinciding with the energies of the noninteracting π^*(C═O) orbitals. The second of these transitions, O1s $\rightarrow$ π^*_-(C═O) should gain less intensity than the first, because of the electronic relaxation screening effect discussed earlier. On the basis of the relative proximity of the two carbonyl groups only, the conjugated π interaction should result in a larger π^*_+(C═O)$-$$\pi^*_-$(C═O) energy splitting in PPDO than in the quinone molecule. This trend has been experimentally verified for the $\pi_+-\pi_-$ energy splitting of the occupied molecular orbitals in dicarbonyls by means of photoelectron spectroscopy;[38] averaged splittings of 2 and 0.3 eV were observed for a set of investigated α- and γ-dicarbonyl molecules, respectively. The carbonyl groups in the pBQ molecule interact with each other through the involvement of the diene groups. Experimentally, this effect can be observed by comparing the $\pi_+-\pi_-$, ~0.2 eV vs 0.3 eV,[38] energy splitting in the quinoid pBQ and 1,4-cyclohexanedione molecules that have a saturated and unsaturated backbone intercalating the two carbonyl groups. With regard to the virtual orbital space, no $\pi^*_+-\pi^*_-$ energy splitting could be observed at the O1s NEXAFS spectrum of 1,4-cyclohexanedione.[27]

4. Summary

In this study, we explored the role of weak molecular orbital interactions and their manifestations in the NEXAFS spectra of small non-conjugated diene molecules. The NEXAFS spectrum of pBQ was used as a reference for molecules with strong conjugated π^* orbital systems. The C1s and O1s NEXAFS spectra of 1,4-cyclohexadiene, norbornadiene, norbornadienone, and [4,4,2]propella-3,8-diene-11,12-dione have been calculated and analyzed for this purpose using two different methods, Hartree$-$Fock and density functional theory. These spectra give direct information about the contribution of different chromophores to unoccupied orbitals and shed light on the character of interactions of the non-conjugated π^* ethylenic orbitals. The hyper-conjugative orbital interaction in CHD is recognized in the methylene C1s NEXAFS channel by the medium-intensity σ^*(C$-$C; CH_2) peak that is pushed below the IP(C═C) ionization threshold. For NBDO and NBDO molecules, a second weak transition arises in the C1s(C═C) partial spectrum that is a spectral signature of a diene through-space orbital interaction. In PPDO, no direct or indirect diene orbital interactions are seen in any C1s partial NEXAFS spectra because of the large separation between these chromophores. Only within the stronger interacting α-dicarbonyl fragments is a conjugative orbital interaction unambiguously observed, here by the red and blue shifts of the C1s(C═O) $\rightarrow$ π^*_+(C═O) and C1s(C═O) $\rightarrow$ π^*_-(C═O) transitions, respectively. By means of these examples, we have shown that NEXAFS spectroscopy offers a new way to detect and characterize through-space and through-bond interactions.

Acknowledgment. This work was supported by the Swedish Research Council (VR). V.C.F. acknowledges financial support from Conselho Nacional de Desenvolvimento Científico e Tecnológico (CNPq) and Coordenação de Aperfeiçoamento de Pessoal de Nível Superior (CAPES) (Brazil).

References and Notes

(1) Stöhr, J. *NEXAFS Spectroscopy*; Springer Series in Surface Science; Springer: Berlin, 1992.

(2) Plashkevych, O.; Yang, L.; Vahtras, O.; Ågren, H. *Chem. Phys.* **1997**, *222*, 125.

(3) Carravetta, V.; Plashkevych, O.; Ågren, H. *J. Chem. Phys.* **1998**, *109*, 1456.

(4) Hoffmann, R. *Acc. Chem. Res.* **1971**, *4*, 1.

(5) Martin, H.-D.; Mayer, B. *Angew. Chem., Int. Ed. Engl.* **1983**, *22*, 283.

(6) Bischof, P.; Hashmall, J. A.; Hellbronner, E.; Hornung V. *Helv. Chem. Acta* **1969**, *52*, 1745.

(7) Paddon-Row, M. N. *Acc. Chem. Res.* **1994**, *27*, 18.

(8) Damle, P.; Ghosh, A. W.; Datta, S. *Chem. Phys.* **2002**, *281*, 171.

(9) Dougherty, D.; Bloomfleld, J. J.; Newkome, G. R.; Arnett, J. F.; McGlynn, S. P. *J. Phys. Chem.* **1976**, *80*, 2212.

(10) Mackenzie-Ross, H.; Brunger, M. J.; Wang, F.; Adcock, W.; Trout, N.; McCarthy, I. E.; Winkler, D. A. *J. Electron Spectroc. Relat. Phenom.* **2002**, *123*, 389.

(11) Takahashi, M.; Ogino, R.; Udagawa, Y. *Chem. Phys. Lett.* **1998**, *288*, 714.

(12) Stephen, T. M.; Burrow, P. D. *Chem. Phys. Lett.* **1991**, *179*, 252.

(13) Merchán, M.; Serrano-Andrés, L.; Slater, L-S.; Roos, B. O.; McDiarmid, P.; Xing, X. *J. Phys. Chem. A* **1999**, *103*, 5468.

(14) Galasso, V. *Chem. Phys.* **1989**, *138*, 231.

(15) Falcetta, M. F.; Jordan, K. D. *J. Am. Chem. Soc.* **1991**, *113*, 2903.

(16) Roos, B. O.; Merchán, M.; McDiarmid, R.; Xing, X. *J. Am. Chem. Soc.* **1994**, *116*, 5927.

(17) Ågren, H.; Carravetta, V.; Vahtras, O.; Pettersson, L. G. M. *Chem. Phys. Lett.* **1994**, *222*, 75.

(18) Helgaker, T.; Jensen, H. J. Aa.; Jørgensen, P.; Olsen, J.; Ruud, K.; Ågren, H.; Auer, A. A.; Bak, K. L.; Bakken, V.; Christiansen, O.; Coriani, S.; Dahle, P.; Dalskov, E. K.; Enevoldsen, T.; Fernandez, B.; Hättig, C.; Hald, K.; Halkier, A.; Heiberg, H.; Hettema, H.; Jonsson, D.; Kirpekar, S.; Kobayashi, R.; Koch, H.; Mikkelsen, K. V.; Norman, P.; Packer, M. J.; Pedersen, T. B.; Ruden, T. A.; Sanchez, A.; Saue, T.; Sauer, S. P. A.; Schimmelpfenning, B.; Sylvester-Hvid, K. O.; Taylor, P. R.; Vahtras, O. *DALTON, A Molecular Electronic Structure Program*, release 1.2, 2001. See http://www.kjemi.uio.no/software/dalton/dalton.html.

(19) Casida, M. E.; Daul, C.; Goursot, A.; Koester, A.; Pettersson, L. G. M.; Proynov, E.; St-Amant, A.; Salahub, D. R.; Duarte, H.; Godbout, N.; Guan, J.; Jamorski, C.; Leboeuf, M.; Malkin, V.; Malkina, O.; Nyberg, M.; Pedocchi, L.; Sim, F.; Triguero, L.; Vela, A. *DEMON-KS*, version 4.0; DeMon Software, 1997.

(20) Krishnan, R.; Binkley, J. S.; Seeger, R.; Pople, J. A. *J. Chem. Phys.* **1980**, *72*, 650.

(21) Yang, L.; Ågren, H.; Carravetta, V.; Pettersson, L. G. M. *Phys. Scr.* **1996**, *54*, 614.

(22) Perdew, J. P.; Wang, Y. *Phys. Rev. B* **1986**, *33*, 8822.

(23) Becke, A. D. *Phys. Rev. A* **1988**, *38*, 3098.

(24) Kutzelnigg, W.; Fleischer, U.; Schindler, M. *NMR Basic Principles and Progress*; Springer-Verlag: Heidelberg, 1990; Vol. 23.

(25) Jordan, K. D.; Michejda, J. A.; Burrow, P. D. *Chem. Phys. Lett.* **1976**, *42*, 227.

(26) Modelli, A.; Burrow, P. D. *J. Phys. Chem.* **1984**, *88*, 3550.

(27) Francis, J. T.; Hitchcock, A. P. *J. Phys. Chem.* **1992**, *96*, 6598.

(28) Bässler, M.; Fink, R.; Buchberger, C.; Väterlein, P.; Jung, M.; Umbach, E. *Langmuir* **2000**, *16*, 6674.

(29) Hitchcock, A. P.; Newbury, D. C.; Ishii, I.; Stöhr, J.; Horsley, J. A.; Redwing, R. D.; Johnson, A. L.; Sette, F. *J. Chem. Phys.* **1986**, *85*, 4849.

(30) Carravetta, V.; Plashkevych, O.; Ågren, H. *Chem. Phys.* **2001**, *263*, 231.

(31) It is interesting to observe that, if one instead had utilized a STEX potential based on the screened C1s $\rightarrow$ **2**π* core excited-state optimized molecular orbitals, it would imply a pBQ C1s NEXAFS spectrum with less intensity given to the C1s(C═C) $\rightarrow$ **1**π* transition as compared to the C1s(C═O) $\rightarrow$ **2**π* core excitation. This is because the LUMO **1**π* virtual orbital entails more contribution from the C═C center, whereas within the working approximation, **2**π* is a rather pure C═O molecular orbital. The converse should be observed for the C1s(C═O) core excitation.

(32) Hitchcock, A. P.; Mancini, D. C. *J. Electron Spectrosc. Relat. Phenom.* **1994**, *67*, 1.

(33) Farren, R. E.; Sheehy, J. A.; Langhoff, P. W. *Chem. Phys. Lett.* **1991**, *177*, 307.

(34) Haack, N.; Ceballos, G.; Wende, H.; Baberschke, K.; Arvanitis, D.; Ankudinov, A. L.; Rehr, J. J. *Phys. Rev. Lett.* **2000**, *84*, 614.

(35) Zhu, P.; Tang, J.; Cau, S. *J. Electron Spectrosc. Relat. Phenom.* **2003**, *129*, 27.

(36) Doomes, E. E.; McCarley, R. L.; Poliakoff, E. D. *J. Chem. Phys.* **2003**, *119*, 4399.

(37) Modelli, A.; Martin, H.-D. *J. Phys. Chem.* **2002**, *106*, 7271.

(38) Dougherty, D.; Brint, P.; McGlynn, S. P. *J. Am. Chem. Soc.* **1978**, *100*, 5597.